HHS Public Access

Author manuscript

Adv Mater. Author manuscript; available in PMC 2017 January 06.

Published in final edited form as:

Adv Mater. 2016 January 06; 28(1): 40–49. doi:10.1002/adma.201503255.

Highly elastic and conductive human-based protein hybrid hydrogels

Prof. Nasim Annabi[†],
Biomaterials Innovation Research Center, Department of Medicine, Brigham and Women's Hospital, Harvard Medical School, Cambridge, MA 02139, USA

Harvard-MIT Division of Health Sciences and Technology, Massachusetts Institute of Technology, Cambridge, MA 02139 USA

Wyss Institute for Biologically Inspired Engineering, Harvard University, Boston, MA, 02115, USA

Department of Chemical Engineering, Northeastern University, Boston, MA, 02115-5000, USA

Dr. Su Ryon Shin[†],
Biomaterials Innovation Research Center, Department of Medicine, Brigham and Women's Hospital, Harvard Medical School, Cambridge, MA 02139, USA

Harvard-MIT Division of Health Sciences and Technology, Massachusetts Institute of Technology, Cambridge, MA 02139 USA

Wyss Institute for Biologically Inspired Engineering, Harvard University, Boston, MA, 02115, USA

Dr. Ali Tamayol,
Biomaterials Innovation Research Center, Department of Medicine, Brigham and Women's Hospital, Harvard Medical School, Cambridge, MA 02139, USA

Harvard-MIT Division of Health Sciences and Technology, Massachusetts Institute of Technology, Cambridge, MA 02139 USA

Wyss Institute for Biologically Inspired Engineering, Harvard University, Boston, MA, 02115, USA

Mr. Mario Miscuglio,
Biomaterials Innovation Research Center, Department of Medicine, Brigham and Women's Hospital, Harvard Medical School, Cambridge, MA 02139, USA

Harvard-MIT Division of Health Sciences and Technology, Massachusetts Institute of Technology, Cambridge, MA 02139 USA

Mr. Mohsen Afshar,
Biomaterials Innovation Research Center, Department of Medicine, Brigham and Women's Hospital, Harvard Medical School, Cambridge, MA 02139, USA

Harvard-MIT Division of Health Sciences and Technology, Massachusetts Institute of Technology, Cambridge, MA 02139 USA

[*]Corresponding authors: A. Khademhosseini, alik@rics.bwh.harvard.edu.
[†]N. Annabi and S.R. Shin contributed equally to this work.

Dr. Alexander Assmann,
Biomaterials Innovation Research Center, Department of Medicine, Brigham and Women's Hospital, Harvard Medical School, Cambridge, MA 02139, USA

Harvard-MIT Division of Health Sciences and Technology, Massachusetts Institute of Technology, Cambridge, MA 02139 USA

Department of Cardiovascular Surgery, Heinrich Heine University, 40225 Duesseldorf, Germany

Dr. Pooria Mostafalu,
Biomaterials Innovation Research Center, Department of Medicine, Brigham and Women's Hospital, Harvard Medical School, Cambridge, MA 02139, USA

Harvard-MIT Division of Health Sciences and Technology, Massachusetts Institute of Technology, Cambridge, MA 02139 USA

Prof. Jeong-Yun Sun,
Department of Material Science and Engineering, Seoul National University, Seoul 151-742, South Korea

Prof. Suzanne Mithieux,
School of Molecular Bioscience, University of Sydney, Sydney, 2006, Australia

Mr. Louis Cheung,
Department of Chemistry, University of Waterloo, Waterloo, Ontario N2L 3G1, Canada

Prof. Xiaowu (Shirley) Tang,
Department of Chemistry, University of Waterloo, Waterloo, Ontario N2L 3G1, Canada

Prof. Anthony S. Weiss, and
School of Molecular Bioscience, University of Sydney, Sydney, 2006, Australia

Prof. Ali Khademhosseini*
Biomaterials Innovation Research Center, Department of Medicine, Brigham and Women's Hospital, Harvard Medical School, Cambridge, MA 02139, USA

Harvard-MIT Division of Health Sciences and Technology, Massachusetts Institute of Technology, Cambridge, MA 02139 USA

Wyss Institute for Biologically Inspired Engineering, Harvard University, Boston, MA, 02115, USA

Department of Physics, King Abdulaziz University, Jeddah 21569, Saudi Arabia

Keywords

Tropoelastin; Graphene oxide; Cardiac tissue engineering; Hydrogel; Elasticity

Elastomers are key components of many natural systems including organisms' organs. In addition, elastomeric polymer-based materials have been used for various applications such as tissue engineering scaffolds[1, 2], drug delivery vehicles[3], models for biological studies[4], and substrates for engineering flexible electronics[5], actuators[6], and sensors[7]. Although synthetic or derived elastomers such as poly(glycerol sebacate) (PGS)[1] and

polyurethanes (PU)[8] based scaffolds are stretchable and tough, they lack the bioactivity of natural elastomers. A key component of the native extracellular matrix (ECM) in elastic tissues is elastin. Thus, many researchers have tried to create biomimetic elastin-based elastomers for applications that require matrix bioactivity. For example, naturally derived elastomeric hydrogels such as elastin-like polypeptide (ELP) gels[9], chemically crosslinked tropoelastin gels[10], photocrosslinkable tropoelastin gels[11, 12], and animal derived elastin gels[13, 14] have been developed for biomedical applications. Although these biomimetic materials are highly elastic, their low toughness makes them unsuitable for many tissue engineering and regenerative medicine applications. Thus, several research groups have attempted to combine natural and synthetic materials to form composite elastomers with high extensibility and toughness such as nanocomposite hydrogels[15], polyrotaxane gels[16], double network (DN) gels[17], hydrophobic bilayers (PDGI)/polyacrylamide (PAAm)[18], and PAAm/alginate composite gels[19]. The limitations of these systems include their permanent deformation, cytotoxicity, and harsh fabrication processes. These characteristics can limit their applicability for biological applications.

The aim of this study is to engineer a biocompatible and stretchable hydrogel with tunable mechanical, electrical, and biological properties based on recombinant human tropoelastin and graphene oxide (GO) nanoparticles. Tropoelastin is the dominant physiological component of elastin, where upon crosslinking it conveys both elasticity and biological activity[20]. Tropoelastin has been used in different forms in various biomedical applications. For example, the methacryloyl-substituted tropoelastin (MeTro) has been developed as a photocrosslinkable elastomer with excellent biocompatibility[11, 12] and remarkable extensibility up to 400%[12]. However, the elastic modulus of MeTro is limited to the range of 2.8 – 14.8 kPa. In addition, similar to the majority of hydrogels and polymeric elastomers, MeTro is electrically non-conductive.

Previous studies have attempted to engineer conductive hydrogels through incorporation of nanomaterials such as gold nanowires[21] and carbon nanotubes (CNTs)[22] within hydrogel networks made of natural or synthetic polymers. Although the incorporation of these nanomaterials improved the elastic modulus and toughness of the engineered hydrogels, their elasticity was significantly reduced[23].

Here, we use GO nanoparticles to form conductive and elastomeric MeTro/GO hybrid hydrogels. GO is utilized due to its flexibility, biocompatibility, and ease of dispersion in aqueous solutions[24]. Unlike other nanomaterial/hydrogel systems, the incorporation of GO nanoparticles in MeTro enhanced both elasticity and toughness of the engineered hydrogel due to the unique interactions between tropoelastin polymer chains and nanoparticles. Our approach enabled us to tune the mechanical and electrical properties of the engineered bioelastomers. These injectable, light-activated, highly elastic, and conductive hydrogels with their unique mechanical, electrical, and biological properties can be used for various applications such as engineering cardiac tissue constructs, bioactuators, and flexible electronics.

MeTro/GO hybrid hydrogels were formed in a two-step process: (a) dispersion of GO nanoparticles in a 10% (w/v) MeTro prepolymer solution; (b) UV photocrosslinking of the

MeTro/GO solution to form a hybrid hydrogel (Fig. S1). We obtained a highly elastic MeTro/GO hydrogel with a uniform brown color where no evidence of nanoparticle aggregation was observed, suggesting a homogeneous distribution of GO throughout the hydrogel (Fig. 1a). Both pure MeTro and hybrid hydrogels were easy-to-handle and exhibited high extensibility and stability.

MeTro comprises an asymmetric coil with a protruding “foot” that encompasses the C-terminal cell interaction motif and a methacrylated group at the N-terminus[20] (Fig. 1b). In particular, this coil region accounts for most of the elasticity of MeTro. GO particles form physical crosslinks with MeTro through hydrophobic and electrostatic interactions between the MeTro chains and the GO surfaces (Fig. 1c). A key aim of this study was to homogeneously disperse GO nanoparticles throughout the MeTro solution to form these physical crosslinks while preserving the coiled region of the protein to provide elasticity to the matrix.

In our previous study, we showed that GO nanoparticles were successfully dispersed in prepolymer solutions (e.g. gelatin) by coating the particles with a thin layer of methacryloyl-substituted gelatin (GelMA) at high temperature (80°C) without using toxic surfactant and sonication process[25]. However, this method is not applicable to MeTro-based prepolymer due to its possible denaturation and coacervation at high temperatures[26]. In this study, the GO particles were successfully dispersed in MeTro prepolymer solution by sonication at low temperatures (4°C). The high resolution transmission electron microscope (HRTEM) images showed the morphological differences between bare and MeTro-coated GO nanoparticles, confirming that a thin layer of MeTro polypeptide was uniformly coated on the particle surfaces without particle aggregation (Fig. 1d–e). This is in agreement with the pertinent literature, where the ability of proteins to strongly bind onto GO surface due to the electrostatic attraction, hydrophobic interaction, and H-bonding has been reported.[27] MeTro-coated GO nanoparticles could then easily be dispersed in a 10 %(w/v) MeTro prepolymer solution and the initial coating of the particles significantly reduced the particle-particle interactions and prevented their aggregation. Finally, the coiled regions of MeTro could maintain their unique structures on the surface of GO particles. The large number of the hydrophilic segments of MeTro interact with water and together with the interactions between the hydrophobic segments of its polypeptide chain with GO can effectively coat and separate GO nanoparticles.

The aggregation of particles in a prepolymer solution can introduce weak points in the polymeric network and therefore can reduce the mechanical properties of the resulting hydrogels. To confirm the dispersion of the GO particles in MeTro solution, the overall particle size distributions were assessed using a Zetasizer before and after sonication with MeTro (Fig. S2). The average particle size decreased after coating with MeTro (731.2 ± 71.2 nm) as compared to that of bare particles (1118.5 ± 156.3 nm). This reduction in particle size may be due to cutting or structural damage to GO sheets during the sonication process.

To demonstrate that MeTro/GO hydrogels are useful hybrid materials for tissue engineering applications, it is important to show that enhancing the stiffness of hydrogels through GO incorporation does not affect the favorable characteristics of pure MeTro hydrogel such as

porosity and elasticity.[28] Scanning electron microscopy (SEM) was employed to confirm the porosity and pore morphology of the MeTro/GO hydrogels (Fig. 1f). Hybrid hydrogels possessed a highly porous microstructure consisting of ordered polyhedral cells and a uniform pore size (18.3 ± 7.3 μm) comparable to those observed in pure MeTro hydrogels (23.4 ± 5.8 μm)[12]. In addition, the smooth surface of the pore walls in hybrid hydrogel is evidence for the absence of GO aggregates. The swelling ratio measurement also showed that MeTro/GO hydrogels had a lower swelling ratio than pure MeTro hydrogels (Fig. S3). The pure MeTro hydrogels form a network by covalent crosslinks under UV light (Fig. 1g). By contrast, in hybrid hydrogels, the matrix is formed by both physical (hydrophobic) bonding between GO particles and MeTro molecules and a large number of covalent bonds in the MeTro matrix (Fig. 1h). This combination of physically and covalently crosslinked networks can enhance the elasticity and elastic modulus of the hybrid hydrogels in comparison to pure MeTro hydrogel.

We first studied the effect of UV exposure time on the elastic modulus of the pure MeTro hydrogel to find the optimum time for photopolymerization of MeTro. The modulus of MeTro hydrogel was about 12.6 ± 0.7 kPa after 6 min of UV exposure with no significant changes after that. The elastic modulus was increased to 19.3 ± 0.7 kPa for hybrid hydrogels containing 1 mg/ml GO that were photocrosslinked for 6 min (Fig. 2a, b). In addition, the rupture strain was higher for MeTro/GO sample than for pure MeTro (203 ± 12 % vs 140 ± 18 %). These observations suggest a possible unique interaction between GO nanoparticles and the polymeric network.

In the majority of nanoparticle incorporated hydrogels, the stiffness and toughness of the engineered hybrid is increased through the addition of the nanoparticles[22]. However, the presence of these nanoparticles can affect the polymer network and reduce the extensibility of the network by creating weak points and nanoscale defects. In our system (explained in Fig. 1b) the interactions between MeTro and GO particles appear to enhance both elastic modulus and extensibility. The bridge region of the tropoelastin chain interacts with GO particles through hydrogen bonds and hydrophobic interactions to enhance the mechanical properties of the hybrid networks. These reversible electrostatic and hydrophobic interactions and H-bonding lead to the self-healing and recovery of the hybrid hydrogels[29]. On the other hand, the coiled region of tropoelastin (shown in Fig 1b) preserved the elasticity of the engineered MeTro/GO hydrogels. To qualitatively compare the resilience and recoverability of the engineered hydrogels against torsional stress, the scaffolds were mounted between clamps of an Instron mechanical tester (initial gauge length of 2 cm). Torsion strain was set by controlling the distance between the clamps. While the top clamp was locked, the bottom one was rotated for different numbers of rounds. After each experiment, the elasticity of the hydrogel was checked by rotating back the samples to its original position and measuring the length and width of the sample to evaluate its plastic deformation. The MeTro/GO gel was capable of withstanding dramatic torsional stress without a plastic deformation (Fig. 2c), exhibiting extraordinary ductility and flexibility. The hybrid hydrogel did not go under plastic deformation after 23 ± 5 rotations and was fully elastic for the rotation; however, pure MeTro gel deformed after the first few rounds and ruptured after 15 ± 4 rotations (Videos S1 and S2). SEM images of the twisted MeTro/Go sample (Fig. 2e) showed that its surface was wrinkled (rumpled) without the formation of

cracks. The excellent flexibility and high resistance to torsion in MeTro/GO hydrogels prevented the occurrence of breakage on the surface of the hydrogels. During the torsional deformation, twisted samples experience both compressive and tensile stresses in different directions. Under tension (indicated by blue arrows in Fig. 2d) a monomer detaches from a particle surface to relax the applied tension. This monomer can be replaced by another monomer belonging to the same or a different polymeric chain to reorganize the network upon compression (indicated by red arrows in Fig 2d). Such continuous reorganization process induces a self-healing characteristic in the network and enhances the energy dissipation. Similar mechanisms has been proposed for explaining the resistance of rubber to fracture[30] and the high elasticity of tough hydrogels containing clay nanoparticles[31].

To investigate the resilience of the engineered hydrogels, cyclic tensile tests with a maximum strain of 100% for 1000 cycles were performed. Both the MeTro and hybrid gels exhibited negligible hysteresis after 1000 cycles of loading and unloading (Fig. 3a). The energy loss for pure MeTro and MeTro/GO hydrogels was calculated based on the area between the loading and unloading curve for cycle 1000. As shown in Fig. 3b, MeTro/GO hybrid hydrogels displayed an energy loss of 0.52 kJ/m^3, which is 34 times higher than pure MeTro (0.01 kJ/m^3). Both hydrogels maintained a low hysteresis compared with most conventional hydrogels, which exhibit high hysteresis and permanent deformation after unloading[32]. For example, in a recent study highly stretchable alginate/polyacrylamide hybrid hydrogels showed pronounced hysteresis and permanent deformation[33]. The higher hysteresis in the hybrid hydrogels might be due to the continuous formation and rupture of non-covalent bonds, which absorbs more energy in comparison to pure MeTro.

We also compared the fracture toughness of MeTro/GO hybrid hydrogel with pure MeTro gel. We captured time lapsed video images of the single edge notch test for MeTro/GO hydrogel (Fig. 3c–d). The frame-by-frame images showed that crack propagation significantly slowed down with the addition of GO particles, providing further evidence of the interactions between GO particles and MeTro. Further, the notched MeTro/GO hybrid hydrogel showed higher ultimate strain rate (150%) compared to that of pure MeTro gel (100%) as shown in the fracture curve in Fig. S4. The composite hydrogels also showed a maximum fracture energy of 38.8 ± 0.8 J/m^2, which was 1.6 fold higher than pure MeTro hydrogel (Fig. 3c).

We also performed a fatigue crack growth test for a single-edge notch on the hydrogel subjected to constant maximum strain rate of 50%. We measured the crack opening displacement (F-COD) as a function of applied force for both hybrid and pure hydrogels (Fig. 3e–f). In the hybrid hydrogels, GO particles prevented crack propagation within the hydrogels and the hybrid gels did not break even after 1000 cycles of loading and unloading of the defected samples (Video S4). However, the pure MeTro broke via crack growth after 836 cycles (Video S3). After the fatigue crack propagation test, the crack region of the MeTro/GO hybrid hydrogel was observed by SEM (Fig. 3i). The hybrid hydrogels still possessed a highly porous microstructures consisting of ordered polyhedral cells and a uniform pore size on the root of notch.

These results provide insight into the mechanisms of deformation and energy dissipation in our highly elastic and tough hydrogels. The elasticity and energy dissipation of MeTro depends on the interactions between water molecules and hydrophobic domains in tropoelastin. Upon stretching the pore sizes and the distance between hydrophobic domains reduce, which can remove the water molecules from the structure and deforming the gel without affecting the polymer network. Upon removal of the applied stress, the polymer chains push the hydrophobic regions and simultaneously water molecules penetrations restore the morphological features. However, when a cracked MeTro hydrogels is stretched, crack propagation can affect the polymer network (Fig.3g). The pure MeTro gel is more notch-sensitive because energy is dissipated over a highly localized region with only a small fraction of the chains in the network participating in energy dissipation. However, in the hybrid gel, the number of chains that participate in energy dissipation is dramatically increased. In addition, GO particles have a high elastic modulus and have been used as reinforcing agents to create porous hydrogels with tunable mechanical properties. Therefore, when a notched hybrid hydrogel is stretched, the propagation of notch was stopped by the GO particles in hybrid hydrogel (Fig. 3h). This was likely the result of the efficient energy transfer between the nanoparticles and MeTro networks, due to their direct coupling, that led to homogeneously distributed GO particles in a large zone being subjected to stress. The load sharing of the MeTro networks and nanoparticles might also have been achieved by entanglements of the MeTro chain on the surface of GO, and by possible covalent crosslinks formed between the acrylic groups on MeTro matrix and MeTro-coated GO particles. Therefore, the incorporation of homogeneously distributed GOs in the macroporous MeTro hydrogel yielded an increase in toughness due to high densities of physical and covalent crosslinks on the surface of GO particles.

To investigate the effect of nanoparticles on the local and global conductivity of the hybrid hydrogels, a thin layer (<5μm) of MeTro and MeTro/GO samples were spin-coated on indium tin oxide (ITO) glass slides. In addition, we created composite samples containing reduced GO (rGO), which was expected to offer higher electrical conductivity. A conductive atomic force microscopy (AFM) analysis was carried out to determine the morphology and local electrical conductance of the samples. As shown in Fig. 4a, MeTro samples showed a uniform topography, while the samples containing GO and rGO showed uneven surface topography, which was due to the presence of nanoparticles on the surfaces of the hydrogels. Simultaneously, by applying a voltage bias in the range of −1 to 1V, the electrical current passing through the sample was measured. We noticed a few locations where a detectable current passed through the composite samples and these locations coincided with the peaks on the surface topography plots. This observation suggests that the incorporated nanoparticles allow electron transfer through the thickness of the sample, while MeTro acted as an electrical insulator. Similar observation was reported for a hybrid alginate/gold nanowire sheet[21]. Another interesting observation was that the current peaks were more pronounced in samples containing rGO, which was expected, as rGO is more electrically conductive than GO.

We also measured the overall film impedance of pristine MeTro and hybrid hydrogels (Fig. 4b). The samples were sandwiched between two Au glass slides and AC bias was applied in the range of 1 Hz to 1 kHz. We found that at lower frequencies, which resembled the

electrophysiological activity of muscular tissue, the composite hydrogels offered lower impedance. Similar to the conductive AFM data, the samples containing rGO had the lowest impedance over the entire frequency range.

A key advantage of the engineered electrically conductive hybrid hydrogel is its capacity for conducting electrical current through biological samples. To assess this phenomenon, abdominal muscle tissues were explanted from rats, cut into square pieces (10 mm×10 mm), and placed in an electrically insulated PDMS mold ~1000 μm apart. Pure MeTro or hybrid hydrogel was then injected in the gap between the tissues and then photocrosslinked as described previously (Fig. 4c). The hydrogel could connect the pieces together and act as a glue (Fig. 4d). We then connected each muscle piece to an electrode and applied a DC electrical voltage to the tissues. The beating or contraction of the muscles was checked and the applied voltage was increased until the muscles contracted (Fig. 4e and Video S5). We observed a lower threshold for muscular tissue connected with hybrid hydrogels compared to the tissues linked with pure MeTro gel. In addition, the electrical threshold for muscular stimulation was lower when MeTro/rGO was used as a connector between tissues compared to MeTro/GO, confirming the higher conductivity of hybrid hydrogels containing rGO. Due to the large thickness of the applied hydrogel layer, this observation suggests a positive role of the nanoparticles on the global conductivity of the composite materials.

Normal function of muscular cells and engineered tissues requires a scaffold that can mimic *in vivo* mechanical and electrical properties. Here, we used the engineered hybrid hydrogel to assess the growth and function of neonatal rat cardiomyocytes (CMs) and cardiac fibroblasts (CFs). We found that both pure and hybrid hydrogels supported the attachment and growth of CFs (Fig. S5) and CMs (Fig. S6). CF spreading and proliferation was promoted in hybrid hydrogels containing higher concentration of GO (Fig. S5). Similarly, higher number of CMs attached to hybrid hydrogels on day 1 and the surfaces of hydrogels were completely covered with CMs by day 7 of culture as shown by SEM and F-actin stained images (Fig. S6a, b). After one day of culture, the average cell area of 559 ± 57 μm^2 on MeTro/GO (2 mg/ml) was twice that on pure MeTro (315 ± 40 μm^2) (Fig. 4g). The proliferation of CMs culture on pure and hybrid hydrogels did not drop over 7 days of culture, confirming the cytocompatibility of the hybrid hydrogels (Fig. S6c). These observations are in line with the previous studies reporting strong cellular adhesion and proliferation on nanomaterials incorporated ECM-based hydrogels[22, 25].

Immunohistochemical analyses demonstrated the maturation of CMs cultured on both pure and hybrid hydrogels after 7 days of culture (Fig. 4f and Fig. S7). Expression of troponin I, sarcomeric α-actinin, and connexin-43 was higher on MeTro/GO containing 2 mg/ml GO than pure MeTro and hybrid gel containing 1 mg/ml GO as shown in Fig. 4f and Fig. S7a,b. In addition, sarcomeric α-actinin staining on samples showed that the cells had developed well-aligned sarcomeric structures on hybrid hydrogels containing 2 mg/ml GO (Fig. S7b), which resembled those of native adult rat ventricular myocardium. Quantification of sarcomere alignment demonstrated that GO nanoparticles improved the alignment of the expressed sarcomeres. We also characterized the beating behavior of CMs seeded on the engineered hydrogels (Fig. S8). CMs seeded on MeTro/GO hybrid gels containing higher concentration of GO displayed stronger and synchronized contractions by as early as 3 days

that contrasted with pure MeTro hydrogels (Videos S6 and S7). The beat frequency, quantified between days 3 and 12, varied between 20–85 beats min^{-1} for MeTro depending on GO concentration. The highest frequency of CMs was observed on day 7 on MeTro/GO hydrogels containing 2 mg/ml GO. In addition, for all the samples, beating frequency decreased from day 6 to day 12 of culture.

To study the effect of GO nanoparticle on excitation threshold, we applied square-wave pulse electrical stimulation (less than 15 V) with relatively short duration according to a previous protocol[11]. Cells contracted in synchrony in response to the applied stimulation on all samples, and could be paced using 50 ms pulses of electrical stimulation up to 3 Hz (Video S8). The excitation threshold was lower on hybrid hydrogels in comparison to pure hydrogels at different frequencies (Fig. 4h). For example, at an applied frequency of 2 Hz, the excitation threshold was approximately 2.3-fold lower for the hybrid gel with 2 mg/ml GO as compared to pure MeTro gel (2.2 V vs. 5 V) ($P < 0.05$). These *in vitro* studies together demonstrated that incorporation of GO particles within the MeTro hydrogel could promote CM growth, proliferation, spreading, phenotype and synchronous beating of CMs. Similar behaviors were observed for CM seeded on GelMA/GO hydrogels[25] and alginate/gold nanowire hydrogels[21]. We believe that the presence of conductive nanoparticles enhances local and nanoscale electrical conductivity and induces cell-cell signaling, which in turn promotes cellular function.

In order to test the *in vivo* biocompatibility of pure and hybrid hydrogels, samples were subcutaneously implanted in rats. Hematoxylin/eosin (H&E) staining after 28 days *in vivo* showed good integration of the samples in the host environment, whereas cellular invasion into the hydrogels was not observed within the short follow-up period (Fig. 4j(i) and 4k(i)). Immunostaining against the lymphocyte marker CD3 did not result in substantially positive signals in any group (Fig. 4j(ii) and 4k(ii)), while there was moderate macrophage infiltration in the subcutaneous tissue around the implants of both groups as indicated by positive staining for CD68 (Fig. 4j(iii) and 4k(iii)). Similar observations were seen in histological and immunostaining images from the samples explanted 3 days after implantation (Fig. S9).

Before being considered as conductive implant material, toxic and immunogenic effects of the hydrogels have to be excluded. In the present project, biocompatibility testing in a subcutaneous rat model revealed that MeTro as well as MeTro/GO hydrogels did not induce relevant local inflammation when used as implants. To the best of our knowledge, this is the first report on such an *in vivo* analysis of MeTro-based hydrogels. Moreover, significant biodegradation *in vivo* does not occur within the first 4 weeks. If these hydrogels are used as conductive implants, their slow degradation is beneficial, since the electrical functionality and structural integrity of the grafts should be maintained as long as regenerative tissue has not replaced the implanted scaffold. However, further investigation on the long-term fate of the implanted material seem to be warranted.

In summary, we have developed a human protein based hybrid hydrogel that offers a combination of elasticity, electrical conductivity, and bioactivity. The hybrid materials were formed by incorporating GO nanoparticles into a highly elastic MeTro-based hydrogel.

Different from other nano-hybrid systems, the incorporation of nanoparticles improved both toughness and elasticity of the engineered hydrogels. This was due to a combination of covalent bonds between polymeric chains and hydrophobic, electrostatic interactions, and H-bonds between the polymer chains and GO nanoparticles. Thus, the engineered hybrid material showed a superior resilience against cyclic tensile and torsional forces. In addition, the developed composite material allowed conductance of electrical current and was successfully used for connecting pieces of explanted abdominal muscles. The hybrid hydrogels allowed electrical current to pass through the defective area. These conductive elastomers also supported CM growth and function and enhanced their activity and maturation in comparison to pure MeTro hydrogels. The material was also found to be biocompatible by triggering a low to moderate inflammatory response after implantation in rats. The synthesized conductive and elastomeric materials with their tunable electrical and mechanical properties can be used for a range of tissue engineering and regenerative medicine applications.

Material and methods

Materials

Chemical reagents were purchased from Sigma-Aldrich St. Louis, MO, USA) unless mentioned otherwise. Methacryloyl-substituted tropoelastin (MeTro) with 44% methacrylation degree was prepared according to procedures explained in our previous studies[11, 12]. Briefly, 15 %(v/v) methacrylate anhydride (MA, Sigma) was added to a 10 % (w/v) tropoelastin solution (Synthetic Human Elastin without domain 26A, recombinant human tropoelastin isoform SHELdelta26A) in phosphate buffered saline (PBS, Invitrogen). The solution was reacted for 12 h at 4°C and then diluted and dialyzed using Slide-A-Lyzer MINI, 3.5K MWCO against water at 4°C for 48 h. The MeTro prepolymer solution was then filtered and lyophilized for further use. The methacrylation of tropoelastin was confirmed by performing ^{1}H NMR analysis as previously described[12].

Preparation of MeTro/GO hybrid hydrogel fabrication

To form MeTro/GO hydrogels, we first dispersed GO nanoparticles in MeTro prepolymer solution in PBS. GO was obtained from graphite following modified Hummer's method. To obtain homogenous dispersion of nanoparticles in MeTro, we first coated GO particles with MeTro by sonication (VCX 400, 80 W, 2 s on and 1 s off) of a 1%(w/v) MeTro solution containing 5 mg/ml GO for 1 h in ice bath. A selected amount of this solution was then added to a MeTro solution (10%w/v) containing 0.5% photoinitiator, 2-hydroxy-1-(4-(hydroxyethoxy) phenyl)-2-methyl-1-propanone (Irgacure 2959, CIBA Chemicals), to make prepolymer solutions for gelation, with a final concentration of GO at 0, 1, and 2 mg/ml. To prepare hydrogel film, 10 μl prepolymer solution was placed between two glass coverslips that were separated by a 150 μm spacer and exposed to 6.9 mW cm^{-2} UV light (360–480 nm) for 6 min (optimized UV exposure time to fully polymerized the hydrogels). To confirm the dispersion of the GOs in MeTro solution, we measured the overall particle size distribution of GOs before and after mixing with MeTro (1 mg/mL) by a Zetasizer. High resolution transmission electron microscope (HRTEM) images (Tecnai 12, FEI, Netherlands) were acquired using a charge coupled detector (CCD) camera to observe the

morphology of MeTro coated GO particles. All sample solutions were loaded onto holey carbon film-supported grids with negative staining (Uranyl acetate).

For conductivity experiments, we used reduced GO (rGO) particles. To make rGO, ascorbic acid (L-Ascorbic acid 2-phosphate sesquimagnesium salt hydrate, Sigma-Aldrich, USA) was dissolved in 15 mL of the GO solution. Then, the mixture was placed in a sonicator (Crest Ultrasonics, Model No 275DA, USA) for 60 min. Afterwards, the solution was kept in the oven at 80 °C for 48 h in order to accelerate the reduction process. Then, the solution was dialyzed (dialysis membrane tubing with 12 – 14 kDa molecular weight cutoff) against distilled water for 5 days at room temperature. The rGO solution in PBS was then mixed with MeTro prepolymer solution and subsequently photopolymerized to form MeTro/rGO hydrogels, using similar procedure explained above for the fabrication of MeTro/GO gels.

Supplementary Material

Refer to Web version on PubMed Central for supplementary material.

Acknowledgments

AA acknowledges postdoctoral funding from the German Heart Foundation, Frankfurt, Germany (S/04/12). AK acknowledges funding from the National Science Foundation (EFRI-1240443), IMMODGEL (602694), and the National Institutes of Health (EB012597, AR057837, DE021468, HL099073, AI105024, AR063745). ASW acknowledges funding from the NIH (EB014283), the Australian Research Council, and National Health and Medical Research Council (NHMRC). NA acknowledges a CJ Martin Fellowship from the NHMRC.

References

1. Wang Y, Ameer GA, Sheppard BJ, Langer R. Nat Biotech. 2002; 20:602.Engelmayr GC, Cheng M, Bettinger CJ, Borenstein JT, Langer R, Freed LE. Nat Mater. 2008; 7:1003. [PubMed: 18978786]
2. Chen Q, Liang S, Thouas GA. Progress in Polymer Science. 2013; 38:584.
3. Borcan F, Soica CM, Ganta S, Amiji MM, Dehelean CA, Munteanu MF. Chem Cent J. 2012; 6:87. [PubMed: 22892194] Mithieux SM, Wise SG, Weiss AS. Advanced drug delivery reviews. 2012 In press.
4. Chaudhuri O, Gu L, Darnell M, Klumpers D, Bencherif SA, Weaver JC, Huebsch N, Mooney DJ. Nat Commun. 2015; 6Nam KH, Jamilpour N, Mfoumou E, Wang FY, Zhang DD, Wong PK. Sci Rep. 2014; 4
5. Najafabadi AH, Tamayol A, Annabi N, Ochoa M, Mostafalu P, Akbari M, Nikkhah M, Rahimi R, Dokmeci MR, Sonkusale S, Ziaie B, Khademhosseini A. Advanced Materials. 2014; 26:5823. [PubMed: 25044366] Libanori R, Erb RM, Reiser A, Le Ferrand H, Süess MJ, Spolenak R, Studart AR. Nat Commun. 2012; 3:1265. [PubMed: 23232395] White MS, Kaltenbrunner M, Glowacki ED, Gutnichenko K, Kettlgruber G, Graz I, Aazou S, Ulbricht C, Egbe DAM, Miron MC, Major Z, Scharber MC, Sekitani T, Someya T, Bauer S, Sariciftci NS. Nat Photon. 2013; 7:811.
6. Pei Z, Yang Y, Chen Q, Terentjev EM, Wei Y, Ji Y. Nat Mater. 2014; 13:36. [PubMed: 24292422] Fratzl P, Barth FG. Nature. 2009; 462:442. [PubMed: 19940914]
7. Kim RH, Kim DH, Xiao J, Kim BH, Park SI, Panilaitis B, Ghaffari R, Yao J, Li M, Liu Z, Malyarchuk V, Kim DG, Le AP, Nuzzo RG, Kaplan DL, Omenetto FG, Huang Y, Kang Z, Rogers JA. Nat Mater. 2010; 9:929. [PubMed: 20953185]
8. Fujimoto KL, Tobita K, Guan J, Hashizume R, Takanari K, Alfieri CM, Yutzey KE, Wagner WR. Journal of Cardiac Failure. 2012; 18:585. [PubMed: 22748493] Guelcher SA, Gallagher KM, Didier JE, Klinedinst DB, Doctor JS, Goldstein AS, Wilkes GL, Beckman EJ, Hollinger JO. Acta Biomater. 2005; 1:471. [PubMed: 16701828]

9. Lim DW, Nettles DL, Setton LA, Chilkoti A. Biomacromolecules. 2007; 8:1463. [PubMed: 17411091] MacEwan SR, Chilkoti A. Biopolymers. 2010; 94:60. [PubMed: 20091871]
10. Mithieux SM, Rasko JE, Weiss AS. Biomaterials. 2004; 25:4921. [PubMed: 15109852] Rnjak J, Li Z, Maitz PKM, Wise SG, Weiss AS. Biomaterials. 2009; 30:6469. [PubMed: 19712968]
11. Annabi N, Tsang K, Mithieux SM, Nikkhah M, Ameri A, Khademhosseini A, Weiss AS. Adv Func Mat.
12. Annabi N, Mithieux SM, Zorlutuna P, Camci-Unal G, Weiss AS, Khademhosseini A. Biomaterials. 2013; 34:5496. [PubMed: 23639533]
13. Annabi N, Mithieux SM, Boughton EA, Ruys AJ, Weiss AS, Dehghani F. Biomaterials. 2009; 30:4550. [PubMed: 19500832]
14. Annabi N, Mithieux SM, Weiss AS, Dehghani F. Biomaterials. 2009; 30:1. [PubMed: 18842297]
15. Haraguchi K, Takehisa T. Advanced Materials. 2002; 14:1120.Djonlagić J, Žugić D, Petrović Z. Journal of Applied Polymer Science. 2012; 124:3024.
16. Okumura Y, Ito K. Advanced Materials. 2001; 13:485.
17. Gong JP. Soft Matter. 2010; 6:2583.
18. Haque MA, Kurokawa T, Kamita G, Gong JP. Macromolecules. 2011; 44:8916.
19. Sun JY, Zhao X, Illeperuma WRK, Chaudhuri O, Oh KH, Mooney DJ, Vlassak JJ, Suo Z. Nature. 2012; 489:133. [PubMed: 22955625]
20. Baldock C, Oberhauser AF, Ma L, Lammie D, Siegler V, Mithieux SM, Tu Y, Chow JY, Suleman F, Malfois M, Rogers S, Guo L, Irving TC, Wess TJ, Weiss AS. Proc Natl Acad Sci U S A. 2011; 108:4322. [PubMed: 21368178]
21. Dvir T, Timko BP, Brigham MD, Naik SR, Karajanagi SS, Levy O, Jin H, Parker KK, Langer R, Kohane DS. Nat Nanotechnol. 2011; 6:720. [PubMed: 21946708]
22. Shin SR, Bae H, Cha JM, Mun JY, Chen YC, Tekin H, Shin H, Farshchi S, Dokmeci MR, Tang S, Khademhosseini A. Acs Nano. 2012; 6:362. [PubMed: 22117858]
23. Wang SF, Shen L, Zhang WD, Tong YJ. Biomacromolecules. 2005; 6:3067. [PubMed: 16283728] Lynam C, Moulton SE, Wallace GG. Advanced Materials. 2007; 19:5.Araby S, Meng Q, Zhang L, Zaman I, Majewski P, Ma J. Nanotechnology. 2015; 26:112001. [PubMed: 25705981]
24. Zhang X, Yin J, Peng C, Hu W, Zhu Z, Li W, Fan C, Huang Q. Carbon. 2011; 49:986.Chang Y, Yang ST, Liu JH, Dong E, Wang Y, Cao A, Liu Y, Wang H. Toxicology Letters. 2011; 200:201. [PubMed: 21130147] Sun X, Liu Z, Welsher K, Robinson J, Goodwin A, Zaric S, Dai H. Nano Research. 2008; 1:203. [PubMed: 20216934]
25. Shin SR, Aghaei-Ghareh-Bolagh B, Dang TT, Topkaya SN, Gao X, Yang SY, Jung SM, Oh JH, Dokmeci MR, Tang X, Khademhosseini A. Advanced Materials. 2013; 25:6385. [PubMed: 23996513]
26. Vrhovski B, Jensen S, Weiss AS. Eur J Biochem. 1997; 250:92. [PubMed: 9431995]
27. Mu Q, Liu W, Xing Y, Zhou H, Li Z, Zhang Y, Ji L, Wang F, Si Z, Zhang B, Yan B. The Journal of Physical Chemistry C. 2008; 112:3300.
28. Lutolf MP, Gilbert PM, Blau HM. Nature. 2009; 462:433. [PubMed: 19940913] Nichol JW, Koshy ST, Bae H, Hwang CM, Yamanlar S, Khademhosseini A. Biomaterials. 2010; 31:5536. [PubMed: 20417964]
29. Fang Y, Wang CF, Zhang ZH, Shao H, Chen S. Sci Rep. 2013; 3:2811. [PubMed: 24091865] Phadke A, Zhang C, Arman B, Hsu CC, Mashelkar RA, Lele AK, Tauber MJ, Arya G, Varghese S. Proceedings of the National Academy of Sciences of the United States of America. 2012; 109:4383. [PubMed: 22392977] Tuncaboylu DC, Sari M, Oppermann W, Okay O. Macromolecules. 2011; 44:9.
30. Lake GJ, Thomas AG. Proceedings of the Royal Society of London A: Mathematical, Physical and Engineering Sciences. 1967; 300:108.
31. Wang Q, Mynar JL, Yoshida M, Lee E, Lee M, Okuro K, Kinbara K, Aida T. Nature. 2010; 463:339. [PubMed: 20090750] Haraguchi K, Uyama K, Tanimoto H. Macromolecular Rapid Communications. 2011; 32:1253. [PubMed: 21732467] Carlsson L, Rose S, Hourdet D, Marcellan A. Soft Matter. 2010; 6:3619.Gaharwar AK, Rivera CP, Wu CJ, Schmidt G. Acta Biomaterialia. 2011; 7:4139. [PubMed: 21839864]

32. Tan M, Zhao T, Huang H, Mingyu G. Polymer Chemistry. 2013; 4:6.Sun TL, Kurokawa T, Kuroda S, Ihsan AB, Akasaki T, Sato K, Haque MA, Nakajima T, Gong JP. Nature materials. 2013; 12:932. [PubMed: 23892784] Yue Y, Kurokawa T, Haque MA, Nakajima T, Nonoyama T, Li X, Kajiwara I, Gong JP. Nature communications. 2014; 5:4659.

33. Sun JY, Zhao X, Illeperuma WR, Chaudhuri O, Oh KH, Mooney DJ, Vlassak JJ, Suo Z. Nature. 2012; 489:133. [PubMed: 22955625]

34. Rivlin RS, Thomas AG. Journal of Polymer Science. 1953; 10:291.

35. Assmann A, Zwirnmann K, Heidelberg F, Schiffer F, Horstkotter K, Munakata H, Gremse F, Barth M, Lichtenberg A, Akhyari P. Biomaterials. 2014; 35:7416. [PubMed: 24917029]

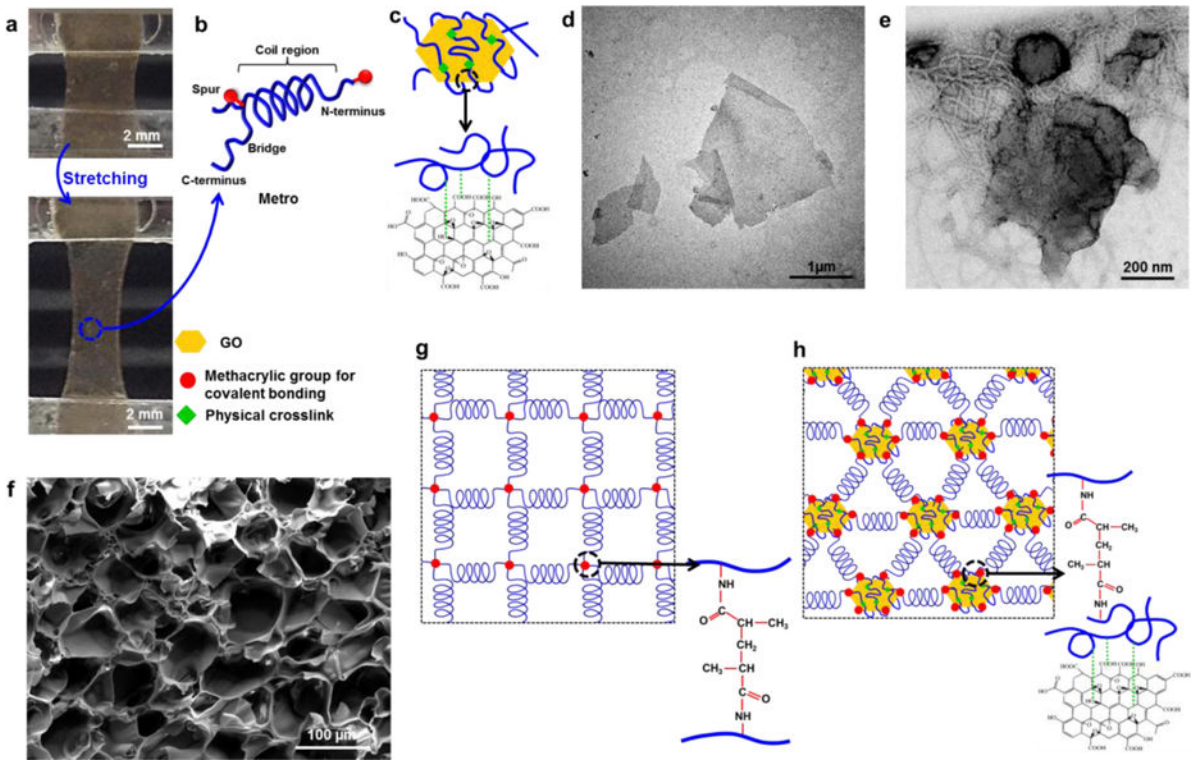

Figure 1.

Formation of MeTro/GO hybrid hydrogel. (a) Representative images from highly elastic MeTro/GO hydrogel before and after stretching formed by using 1 mg/ml GO and 10 % (w/v) MeTro prepolymer solution. (b) Extensible MeTro molecule with an asymmetric coil and a C-terminal cell interactive motif. (c) GO particles coated by MeTro solution for the formation of hydrophobic bonding between GO particles and MeTro. HRTEM images from (d) GO particles in PBS and (e) MeTro-coated GO particles in PBS, showing that tropoelastin fibers presented in MeTro covered the particles. (f) Representative SEM image from a highly porous structure of MeTro/GO hybrid gel. (g) UV photocrosslinked MeTro hydrogel network formed by covalently bonding of MeTro molecules during UV crosslinking. (h) MeTro/GO hydrogel network created by both covalently bonding due to UV crosslinking and physical (hydrophobic) bonding between GO particles and MeTro molecules.

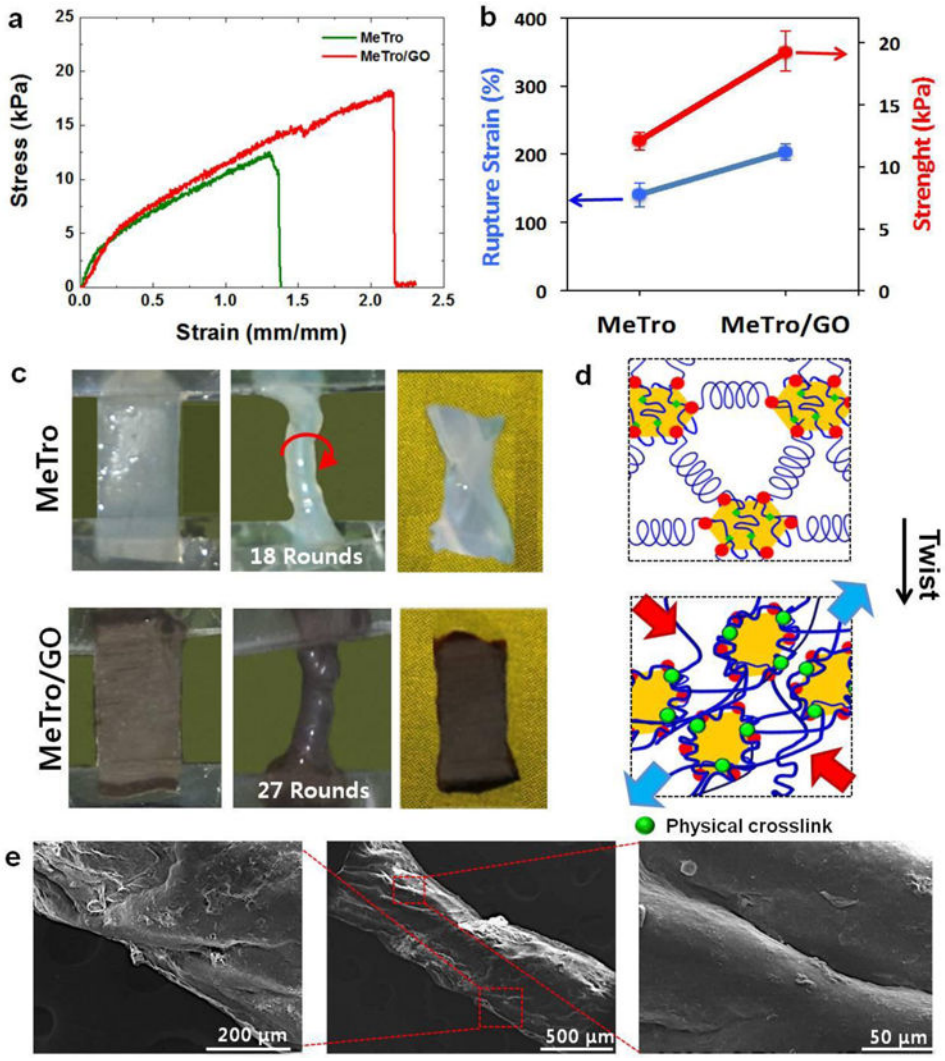

Figure 2. Mechanical characterizations of MeTro/GO hybrid hydrogels under tension and torsion

(a) Stress–stretch curves of pure MeTro and MeTro/GO hydrogels photocrosslinked after 6 min exposure to UV light (MeTro concentration: 10 %(w/v), GO: 1 mg/ml). (b) Rupture strain and ultimate strength for MeTro and MeTro/GO, demonstrating that the addition of GO particles increased both the extensibility and ultimate strength of MeTro hydrogel. (c) Images of MeTro and MeTro/GO hydrogels under torsion test (left panel: before the test, middle image: during the test, right image: recovered gel after 10 rounds), significant deformation was observed after 10 times twisting for MeTro gel as compared with no deformation for MeTro/GO gel. (d) Schematic illustration of the network structure of the hybrid gel before and after twisting, demonstrating that the hybrid hydrogels undergo both tension (indicated by blue arrows) and compression (indicated by red arrows) during the torsion test. The presence of MeTro fibers will provide high elasticity without hysteresis as the network is stretched and the GO nanoparticles are anchored to the gel networks through physical bonding and act as connectors as the hydrogel network is compressed. These two processes allow for high resilience and minimal deformation of the hybrid network after the

torsion test. (e) SEM images from the twisted hybrid gel, showing no breakage in the hydrogel structure after twisting.

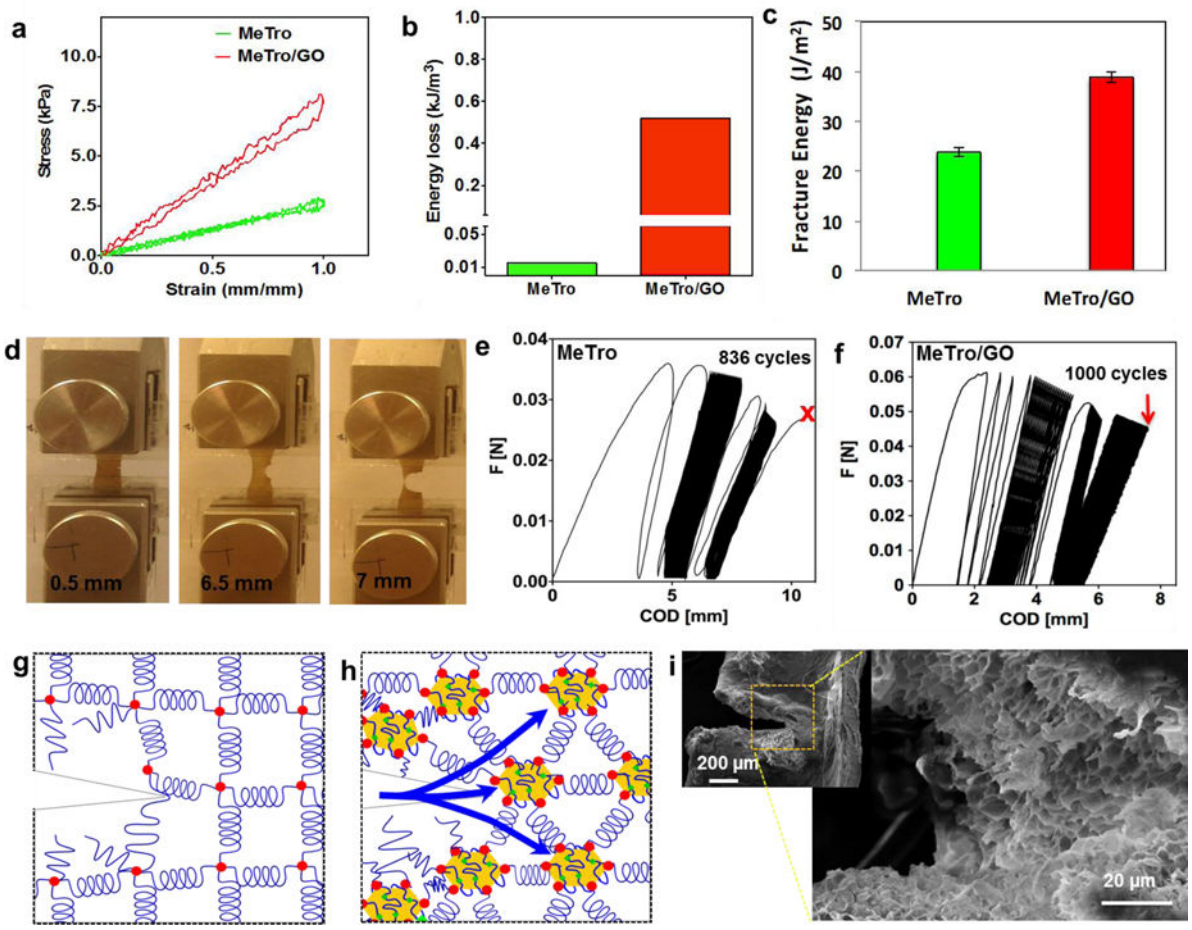

Figure 3.

Cyclic tensile test and crack test on MeTro/GO hybrid gel (MeTro concentration: 10 %(w/v), GO: 1 mg/ml). (a) Stress-strain curves of MeTro and MeTro/GO hydrogels after 1000 cycles of loading and unloading. (b) Energy loss calculated based on the area between loading and unloading curves. (c) Fracture tests for MeTro/GO and MeTro hydrogels. (d) Images from MeTro/GO hydrogel with crack under tension. F-COD curves for (e) MeTro and (f) MeTro/GO hydrogels with cracks, demonstrating that MeTro gel broke from the crack point after 836 cycles of loading and unloading but MeTro/GO hybrid hydrogel underwent more than 1000 cycles (limit of the software) without breakage. (g–h) Schematic illustration of the network structure of the gels during the crack test, showing that crack propagated in the MeTro hydrogel but the presence of GO particles could retard a crack propagation in MeTro/GO hybrid gel. (i) SEM image of MeTro/GO hybrid gel with the crack.

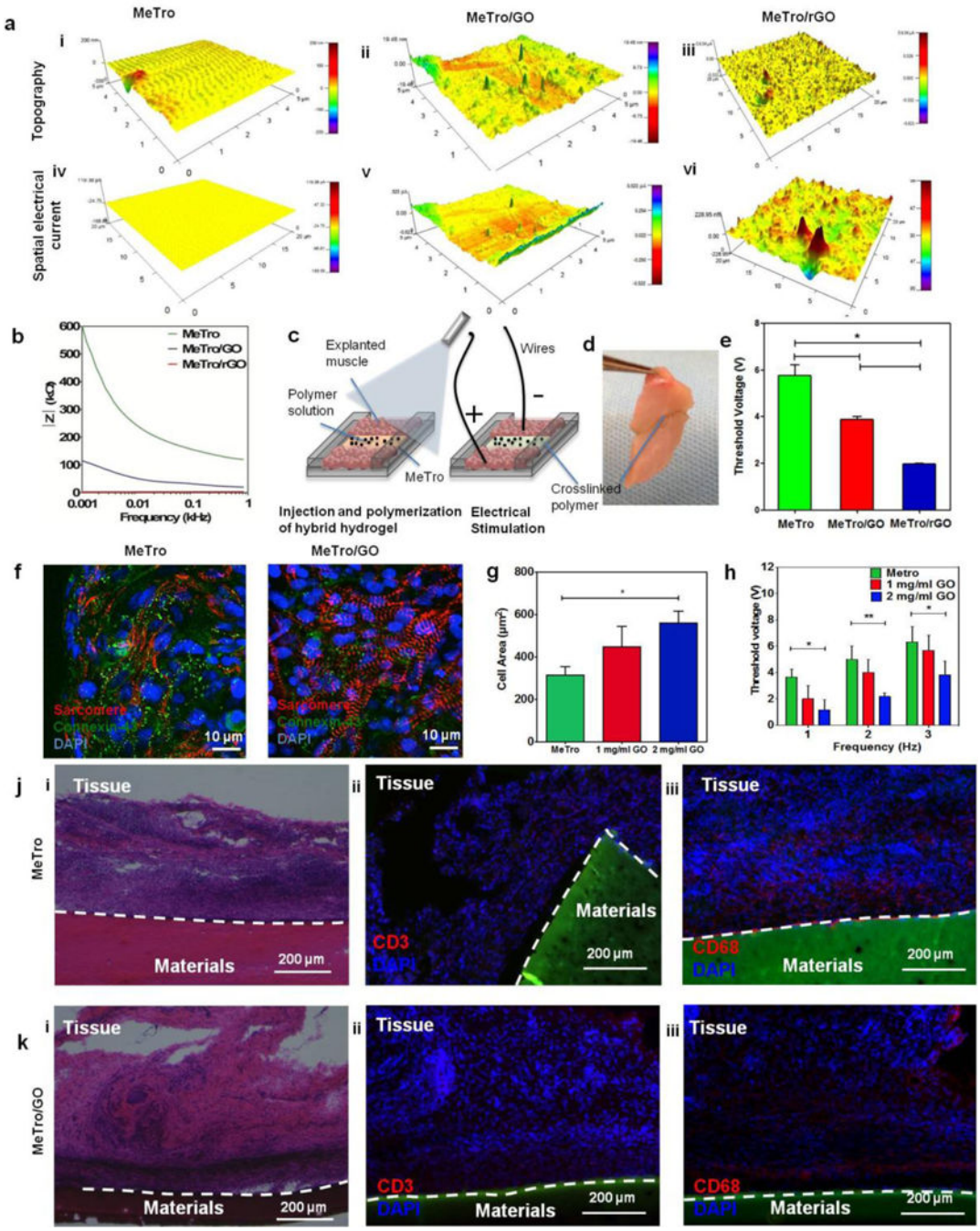

Figure 4.

Electrical and biological characterizations of engineered hydrogels. (a) Spatial topography and conductivity of (i, iv) pure MeTro, (ii, v) MeTro/GO hybrid, and (iii, vi) MeTro/rGO hydrogels, measured by conductive probe atomic force microscopy (C-AFM). Surface topographical mapping shown in (i–iii), confirmed that the presence of nanoparticles changed the surface topography of the hydrogels. Spatial conductivity of hydrogels presented in iv–vi, demonstrates current spikes at the location of nanoparticles in hybrid gels. (b) Overall impedance of pure MeTro and hybrid hydrogels, showing lower electrical

resistance for hybrid hydrogel. (c) The schematic illustration of ex vivo setup used for measuring excitation threshold of muscle. Two pieces of rat abdominal muscles were placed in closed proximately (1 mm apart) and the hydrogels were injected and photopolymerized between the tissues to connect them together. An electrical potential was applied on tissues by using an electrical function generator and the minimum voltage to induce muscle contraction was measured and reported as excitation threshold. (d) Representative image of two pieces of muscle connected with MeTro/GO hybrid gel. (e) Excitation threshold of muscle tissue connected by pure MeTro and hybrid gels, demonstrating that, MeTro/rGO hybrid gels gave rise to the lowest excitation threshold, which was due to the highest conductivity of the MeTro/rGO hybrid gels. (f) Immunostaining for the expression of sarcomeric α-actinin (red)/connexin-43 (green)/nuclei (blue) on CM-seeded pure MeTro and hybrid gels on day 7 of culture. (g) Cell spreading, defined as the area of cell clusters divided by the number of the cells within those cluster, on MeTro, MeTro/GO (1 mg/ml GO), and MeTro/GO (2 mg/ml GO) on day 7 of culture, demonstrating higher cell spreading on MeTro/GO samples compared to MeTro. (h) Excitation threshold of cardiac tissues on MeTro (green), MeTro/GO (1 mg/ml GO) (red), and MeTro/GO (2 mg/ml GO) (blue) at various frequencies. (j, h) Histology and immunohistology images of pure MeTro and MeTro/GO hydrogels 28 days after implantation in the subcutaneous tissue of a rat. H&E images are shown in (i) and immunohistology images of gels stained for CD3 (T-lymphocytes, in red) and CD68 (macrophages, red) are shown in (ii) and (iii), respectively. The immunohistology images confirmed that there were no T-lymphocytes present in any of the explanted samples, confirming the biocompatibility of both the pure and hybrid gels. Error bars represent the SD of measurements performed on 5 samples (*$p < 0.05$, **$p < 0.01$).